Journal of Computational and Applied Mathematics xxx (xxxx) xxx

Contents lists available at ScienceDirect

Journal of Computational and Applied Mathematics

journal homepage: www.elsevier.com/locate/cam

Recovery of bivariate functions from the values of its Radon transform using Laplace inversion

Robert M. Mnatsakanov [a,*], Rafik H. Aramyan [b]

[a] Department of Mathematics, West Virginia University, P.O. Box 6310, Morgantown, WV 26506, USA
[b] Russian-Armenian University, 123 Hovsep Emin Str., Yerevan 0051, Armenia

ARTICLE INFO

Article history:
Received 25 February 2020
Received in revised form 9 March 2021

Keywords:
Approximation of Laplace transform inversion
Approximation of Radon transform inversion
Estimation of the Radon transform

ABSTRACT

The problems of recovering a multivariate function f from the scaled values of its Laplace and Radon transforms are studied, and two novel methods for approximating and estimating the unknown function are proposed. Moreover, using the empirical counterparts of the Laplace transform of the underlying function, a new estimate of the Radon transform itself is obtained. Under smoothed conditions on the underlying function the uniform convergence of the proposed constructions are established, and their accuracy is illustrated graphically with several simple examples.

1. Introduction

The Radon transform and its inverse play a central role in Computed Tomography (CT). Such an inversion is required in problems of thermo- and photo-acoustic tomography, ultrasound reflection tomography, radar imaging, and other areas. Note that, in CT the data represents integrals (projections) of the underlying function over lines, circles, or spheres, based on which the medical image should be reconstructed (see, for example, [1–4], among many others). Thus, in all the above mentioned applications the only available data, provided by the detectors, consists of the values of the Radon transform of the underlying function computed over lines, curves or surfaces.

It is well known that the inverse of the Radon transform is not a continuous operator, and there exist different numerical methods for its approximation, including the very well known filtered back-projection, as well as iterative, and variational approaches. See for example, [2,5–7], and the references therein. Some approximations are based on using the relationship between the moments of the Radon transform $\mathcal{R}f$ and the moments of the underlying function f, see for example, [6,8], and [9]. In [10], a generalized Radon transform on the sphere was considered and a new method to invert this transform was proposed.

In this paper we suggest a method that is based on the relationship between the values of univariate Laplace transform of $\mathcal{R}f$ and the values of the bivariate Laplace transform $\mathcal{L}_f^{(2)}$ of f (the Central Slice Theorem). The approach based on recovering the moments of the unknown function f from the values of its Radon transform is very helpful when the support of f is a compact. See, for example, [9,11,12], and [8]. In the case when the support of f is unbounded we suggest a technique based on the inversion of the Laplace transform instead of recovering a function from its moments. Therefore, we do not need to solve the system of equations that relate the moments of the underlying functions to the moments of its Radon transform; we only need to approximate the inverse of the bivariate Laplace transform of f.

The proposed approach has three main advantages: (a) it provides a computationally stable approximation and is based on a finite number of the scaled values of Laplace and Radon transforms; (b) the suggested approximations admit

* Corresponding author.
E-mail address: Robert.Mnatsakanov@mail.wvu.edu (R.M. Mnatsakanov).

https://doi.org/10.1016/j.cam.2021.113557
0377-0427/

a closed form expression; (c) a regularization procedure is not required as in the case of ill-posed inverse problems (see, for example, [13]).

To describe our construction, let us use the following notation: let $\boldsymbol{\xi}_\theta = (\cos\theta, \sin\theta)', 0 \le \theta \le 2\pi$, be a unit vector in $\mathbb{R}^2$, and $\langle \mathbf{x}, \boldsymbol{\xi}_\theta \rangle$ – the inner product of the vectors $\boldsymbol{\xi}_\theta$ and $\mathbf{x} = (x, y) \in \mathbb{R}^2$. The Radon transform $g = \mathcal{R}f$ of a square-integrable function $f : \mathbb{R}^2 \to \mathbb{R}_+$ is defined as the collection of line integrals

$$\mathcal{R}f(\boldsymbol{\xi}_\theta, t) = \int_{\{\mathbf{x}: \langle \mathbf{x}, \boldsymbol{\xi}_\theta \rangle = t\}} f(\mathbf{x})\, d\, m(\mathbf{x}), \quad (\theta, t) \in (0, 2\pi] \times \mathbb{R}_+, \tag{1}$$

where dm is the arc length measure on the line $\langle \boldsymbol{\xi}_\theta, \mathbf{x} \rangle = t$. Note that in [14] the convergence rate of the estimate of so-called empirical Radon transform and its inversion are derived from knowledge of projections in all directions $\boldsymbol{\xi}_\theta$ in $\mathbb{R}^3$. In our construction one needs to know the projections for a finite number of directions (specified by the number of values of the Laplace or Radon transforms used in the constructions).

The article is organized as follows. In Section 2 we present the well known Central Slice Theorem in terms of the Laplace transform. In Section 3, we obtain a new result regarding uniform convergence for approximated bivariate functions f_a using the scaled values of Laplace transform (cf. with [15] and [8] in the case when the support of f is a compact). In Section 4, two novel approximants as well as estimates of the Radon transform inverse and the Radon transform itself are proposed. It is worth noting that our constructions are based on the scaled values of Laplace transform and provide more accurate approximations compared to the ones that use the values of Laplace transform with an integer argument (cf. with [15]). In Section 5, several simple examples are considered to illustrate the accuracy of the approximations. Here we assumed f to be the probability density of a bivariate distribution F with support in $\mathbb{R}^2_+$, although all statements below are valid for any continuous and bounded function on $\mathbb{R}^2_+$. Finally, in Section 6, several advantages of the proposed constructions are outlined.

2. The central slice theorem in $\mathbf{R}^d$

In this section we use the following notation: by $\mathbb{R}^d$ we denote the d-dimensional Euclidean plane, $\mathbb{R} := \mathbb{R}^1$, and by $\mathbf{S}^{d-1}$ the $(d-1)$th dimensional unit sphere centered at the origin. In addition, the following parametrization of a hyperplane e in $\mathbb{R}^d$, is used: $e = (\boldsymbol{\xi}, p)$, where $p\,(p > 0)$ is the distance from the origin O to e, and $\boldsymbol{\xi} \in \mathbf{S}^{d-1}$ is the directional normal vector to e. Also by $\boldsymbol{\xi}^\perp = \{\mathbf{x} \in \mathbb{R}^d : \langle \mathbf{x}, \boldsymbol{\xi} \rangle = 0\}$ we denote the subspace of $\mathbb{R}^d$ orthogonal to $\boldsymbol{\xi}$.

Definition 1. The multidimensional Laplace transform of $f : \mathbb{R}^d_+ \to \mathbb{R}$ is defined as follows:

$$\mathcal{L}_f^{(d)}(\mathbf{s}) = \int_{\mathbb{R}^d_+} e^{-\langle \mathbf{s}, \mathbf{x} \rangle} f(\mathbf{x})\, d\mathbf{x}, \quad \mathbf{s} = (s_1, s_2, \ldots, s_d) \in \mathbb{R}^d_+ := (0, \infty)^d. \tag{2}$$

Definition 2. The Radon transform of $f : \mathbb{R}^d \to \mathbb{R}$ is defined as follows:

$$\mathcal{R}f(\boldsymbol{\xi}, t) = \int_{\{\mathbf{x}: \langle \mathbf{x}, \boldsymbol{\xi} \rangle = t\}} f(\mathbf{x})\, d\, m(\mathbf{x}) = \int_{\boldsymbol{\xi}^\perp} f(t\boldsymbol{\xi} + \mathbf{y}) d\mathbf{y}, \quad t \in \mathbb{R}, \tag{3}$$

where $\mathbf{y} = (y_1, y_2, \ldots, y_{d-1}) \in \boldsymbol{\xi}^\perp$, $\mathbf{x} = (x_1, x_2, \ldots, x_d)$, and dm represents the Lebesgue measure on the hyperplane $\langle \mathbf{x}, \boldsymbol{\xi} \rangle = t$.

Assuming that the support of f is a subset of $\mathbb{R}^d_+$ one can prove

Theorem 1 (*Central Slice Theorem*). *For any $\sigma \in (0, \infty)$ and $\boldsymbol{\xi} \in \mathbf{S}^{d-1}$, we have*

$$\mathcal{L}^{(1)}_{\mathcal{R}f(\boldsymbol{\xi}, \cdot)}(\sigma) = \mathcal{L}_f^{(d)}(\sigma\, \boldsymbol{\xi}). \tag{4}$$

Proof. After substitution, we have

$$\mathcal{L}^{(1)}_{\mathcal{R}f(\boldsymbol{\xi}, \cdot)}(\sigma) = \int_0^\infty e^{-\sigma u} \mathcal{R}f(\boldsymbol{\xi}, u)\, du = \int_0^\infty e^{-\sigma u} \int_{\boldsymbol{\xi}^\perp} f(u\boldsymbol{\xi} + \mathbf{y})\, d\mathbf{y}\, du. \tag{5}$$

Consider the mapping $(u, \mathbf{y}) := (u, y_1, y_2, \ldots, y_{d-1}) \to (x_1, x_2, \ldots, x_d) := \mathbf{x}$ defined by the following system

$$u\boldsymbol{\xi} + \mathbf{y} = \mathbf{x}.$$

Note that the Jacobian of this transform is $J = 1$, hence, after changing variables in the multiple integrals and taking into account that $u = \langle \boldsymbol{\xi}, \mathbf{x} \rangle$, we get

$$\mathcal{L}^{(1)}_{\mathcal{R}f(\boldsymbol{\xi}, \cdot)}(\sigma) = \int_0^\infty \int_{\boldsymbol{\xi}^\perp} e^{-\sigma \langle \boldsymbol{\xi}, \mathbf{x} \rangle} f(\mathrm{x}) d\mathrm{x} = \mathcal{L}_{f^{(d)}}(\sigma\, \boldsymbol{\xi}). \quad \square \tag{6}$$

Remark 1. A theorem similar to the Central Slice Theorem but expressed in terms of the Fourier transform is also known as the Projection Theorem (see, for example, [2], Theorem 2.1).

In the sequel we restrict ourselves to the case when $d = 2$, although the proposed constructions are valid for $d \geq 3$ as well. The main problem in the latter case is connected to the computational aspect of evaluating the multiple sums presented in the constructions similar to (9). The asymptotic behavior of corresponding approximations will be investigated in a separate paper by applying parallel computing methods.

3. Bivariate Laplace transform inversion

Assume that $d = 2$, $\mathbf{x} = (x_1, x_2)$ and $\mathbf{t} = (t_1, t_2)$. Consider the bivariate Laplace transform of function f scaled by $\ln b$:

$$\mathcal{L}_f^{(2)}(\mathbf{t}\ln b) = \int_{\mathbb{R}_+^2} e^{-\langle \mathbf{t}\ln b, \mathbf{x}\rangle} f(\mathbf{x})\,\mathrm{d}x, \quad \text{for some } b > 1. \tag{7}$$

In the sequel we will use the following notations $\mathcal{L}_{f,b}^{(2)}(\mathbf{t}) := \mathcal{L}_f^{(2)}(\mathbf{t}\ln b)$ and $a = (\alpha, \alpha')$, with $\alpha, \alpha' \in \mathbb{N}_+ = \{1, 2, \ldots\}$. Also, we write $a \to \infty$ to mean that $\alpha \to \infty$ and $\alpha' \to \infty$.

Introducing $\varphi(\mathrm{x}) = (\phi(x_1), \phi(x_2))$, where $\phi(x) = b^{-x}$ for each $x \in \mathbb{R}_+$, let us rewrite (7) in terms of the exponential moments when $\mathbf{t} = (j+1, k+1)$. Multiplying the latter value by $(\ln b)^2$, we define

$$m_\varphi(j,k) := (\ln b)^2\, \mathcal{L}_{f,b}^{(2)}(\mathbf{t})|_{\mathbf{t}=(j+1,k+1)} = (\ln b)^2 \int_0^\infty \int_0^\infty \big[\phi(x_1)\big]^{j+1}\big[\phi(x_2)\big]^{k+1} f(x_1,x_2)\,\mathrm{d}x_1\mathrm{d}x_2, \tag{8}$$

for each $(j,k) \in \mathbb{N}_\alpha \times \mathbb{N}_{\alpha'}$, where $\mathbb{N}_\alpha := \{0, 1, \ldots, \alpha\}$. Consider the following approximation $f_a := \big(\mathcal{B}_a^{-1} m_\varphi\big) \circ \varphi$ of f with

$$\Big(\big(\mathcal{B}_a^{-1} m_\varphi\big) \circ \varphi\Big)(\mathbf{x}) := \frac{\Gamma(\alpha+2)\Gamma(\alpha'+2)}{\Gamma([\alpha\phi(x_1)]+1)\Gamma([\alpha'\phi(x_2)]+1)} \times \sum_{j=0}^{\alpha-[\alpha\phi(x_1)]} \sum_{k=0}^{\alpha'-[\alpha'\phi(x_2)]} \frac{(-1)^{j+k} m_\varphi\big(j+[\alpha\phi(x_1)], k+[\alpha'\phi(x_2)]\big)}{j!k!(\alpha-[\alpha\phi(x_1)]-j)!(\alpha'-[\alpha'\phi(x_2)]-k)!}, \quad \mathbf{x} \in \mathbb{R}_+^2, \tag{9}$$

(cf. with [15], Corollary 4 (iii)). Here, and in a similar formula below, we denote by $[x]$ the largest integer that is less or equal to x. Our goal now is to recover f, given the values of exponential moments $m_\varphi := \{m_\varphi(j,k), (j,k) \in \mathbb{N}_\alpha \times \mathbb{N}_{\alpha'}\}$.

In the proof of the main statement below we suggest the following two-step procedure: in the first step we construct the approximation of a function defined on unit square, and then, in the next step, after a change of variables, we go back to the original function $f : \mathbb{R}_+^2 \to \mathbb{R}$. In what follows, the symbol " $\xrightarrow{u}$ " is used to denote uniform convergence. One can prove the following statement.

Theorem 2. *If the function f is continuous and bounded, then $f_a \xrightarrow{u} f$ as $a \to \infty$.*

Proof. Given the values of $m_\varphi(j,k), (j,k) \in \mathbb{N}_\alpha \times \mathbb{N}_{\alpha'}$, let us recover f using the two-step procedure outlined before Theorem 2. Namely, let us apply the result from [15] and assume that we are given the sequence of moments $m := \{m(j,k), (j,k) \in \mathbb{N}_\alpha \times \mathbb{N}_{\alpha'}\}$ of some continuous bivariate density function $g : [0,1]^2 \to \mathbb{R}_+$ with:

$$m(j,k) := \int_0^1 \int_0^1 t^j s^k\, g(t,s)\mathrm{d}t\,\mathrm{d}s. \tag{10}$$

Now, for each $\mathrm{u} = (u,v) \in [0,1]^2$, consider the approximation $g_a := \mathcal{B}_a^{-1} m$ of g:

$$g_a(\mathrm{u}) := \big(\mathcal{B}_a^{-1} m\big)(\mathrm{u}) = \frac{\Gamma(\alpha+2)\Gamma(\alpha'+2)}{\Gamma([\alpha u]+1)\Gamma([\alpha' v]+1)} \times \sum_{j=0}^{\alpha-[\alpha\,u]} \sum_{l=0}^{\alpha'-[\alpha'\,v]} \frac{(-1)^{j+l} m(j+[\alpha\,u], l+[\alpha'\,v])}{j!l!(\alpha-[\alpha\,u]-j)!(\alpha'-[\alpha'\,v]-l)!}. \tag{11}$$

In Theorem 2 [15] it is proved that g_a converges to g uniformly as $a \to \infty$, under the smooth conditions on g, i.e., when $\alpha, \alpha' \to \infty$. Hence, changing variables under the integral in (8) with $b^{-x_1} = u$ and $b^{-x_2} = v$, gives

$$m_\varphi(j,k) = \int_0^1 \int_0^1 u^{j+1} v^{k+1}\, g(u,v) \frac{\mathrm{d}u}{u}\frac{\mathrm{d}v}{v} = \int_0^1 \int_0^1 u^j v^k\, g(u,v)\mathrm{d}u\,\mathrm{d}v := m(j,k), \tag{12}$$

where

$$g(u,v) = f\big(\phi^-(u), \phi^-(v)\big). \tag{13}$$

Here ϕ^- denotes the inverse function of ϕ.

Now, combining (10)–(13), from the uniform convergence $g_a \xrightarrow{u} g$ it follows:

$$f_a(\mathbf{x}) = g_a(\phi(x_1), \phi(x_2)) \xrightarrow{u} g(\phi(x_1), \phi(x_2)) = f(\mathbf{x}) \quad \text{as} \quad a \to \infty. \quad \square \tag{14}$$

Remark 2. To derive the rate of approximation one needs additional smooth conditions on f. In particular, assuming that the partial derivatives of f up to the second order are bounded and continuous, and the underlying function has a compact support in $\mathbb{R}^2_+$, the rate of convergence was derived in [8]. A similar rate of approximation can be also derived when support of f is unbounded. This question will be a subject of investigation in a separate article.

Remark 3. To approximate the inverse Laplace transform in the univariate case, consider the following scaled values of the Laplace transform

$$m_\phi(j) := (\ln b)\, \mathcal{L}^{(1)}_{f,b}(\mathrm{t})|_{\mathrm{t}=j+1} = (\ln b) \int_0^\infty \big[\phi(x_1)\big]^{j+1} f(x_1)\, \mathrm{d}x_1, \quad \text{for } j = 0, 1, \ldots, \alpha. \tag{15}$$

The approximation is defined as follows:

$$f_\alpha(x_1) := \Big(\big(\mathcal{B}^{-1}_\alpha m_\phi\big) \circ \phi\Big)(x_1) = \frac{\Gamma(\alpha+2)}{\Gamma([\alpha\phi(x_1)]+1)} \sum_{j=0}^{\alpha-[\alpha\phi(x_1)]} \frac{(-1)^j m_\phi\big(j+[\alpha\phi(x_1)]\big)}{j!\,(\alpha-[\alpha\phi(x_1)]-j)!}, \quad x_1 \in \mathbb{R}_+. \tag{16}$$

Furthermore, the following statement is valid:

Corollary 1. *If the univariate function f is continuous and bounded, then $f_\alpha \xrightarrow{u} f$ as $\alpha \to \infty$.*

Remark 4. Note that the constructions (8)–(9) and (15)–(16) are slightly different if compared to ones derived in [15], see Corollary 4 (iii) and Remark 1 in [16], respectively. Namely, in (8) and (15) the arguments of the values of Laplace transforms are shifted by 1. This enables us to avoid using the factors $\phi(x)$ and $\phi(y)$ presented before the summation signs in similar approximations from [15] and [16].

4. Approximating the Radon transform and its inversion

In this section we consider the problem of approximating the bivariate function f from its projections in $\mathbb{R}^2_+$. Namely, using the results from the previous sections we describe the methodology of constructing the approximants and estimates of the Radon transform and its inverse. Their graphical illustrations are provided in Section 5.

4.1. Approximating the inverse of Radon transform

In this section we denote the directional normal vector $\boldsymbol{\xi}$ by $\boldsymbol{\xi}_\theta = (\cos\theta, \sin\theta)$ for some $0 \le \theta \le \frac{\pi}{2}$.

In [8], the connection between the values of the moments of the Radon transform and the moments of the underlying bivariate function f was used to recover an unknown function f from its mollified Radon transform. In this section we apply the Laplace transform technique instead of the one based on the moments. This approach provides stable and very accurate approximations.

To approximate the inverse of the Radon transform, we use the property (see Theorem 1) connecting the Laplace transform of the Radon transform $\mathcal{R}f(\theta, t)$ (with respect to the second argument) and the values of the bivariate Laplace transform of f (see also, [2]). In particular, for the scaled Laplace transform of $\mathcal{R}f$, we have

$$\mathcal{L}^{(1)}_{\mathcal{R}f(\theta,\cdot),b}(\sigma) = \mathcal{L}^{(2)}_{f,b}(\sigma\cos\theta, \sigma\sin\theta), \quad \text{for } 0 \le \theta \le 2\pi \text{ and } \sigma > 0. \tag{17}$$

We then carry out the following steps: For fixed two nonnegative integers, $(j, m) \in \mathbb{N}^2_0$, we evaluate the value of scaled Laplace transform $\mathcal{L}^{(1)}_{\mathcal{R}f(\theta,\cdot),b}(\sigma)$ of $\mathcal{R}f(\theta,\cdot)$, when the pair (θ, σ) represents solution of the following system of equations:

$$\begin{cases} [\sigma\cos\theta] = j+1 \\ [\sigma\sin\theta] = m+1. \end{cases} \tag{18}$$

In other words, we can describe out construction of the Radon inverse as follows:

Step 1: For each fixed (j, m), let $(\sigma_{j,m}, \theta_{j,m})$ be the solution of (18), i.e.,

$$\sigma_{j,m} = \sqrt{(j+1)^2 + (m+1)^2}$$
$$\theta_{j,m} = \arctan\Big(\frac{m+1}{j+1}\Big). \tag{19}$$

Step 2: Evaluate the left hand side of (17) with $(\theta, \sigma) = (\theta_{j,m}, \sigma_{j,m})$, i.e., $\mathcal{L}^{(1)}_{\mathcal{R}f(\theta_{j,m},\cdot),b}(\sigma_{j,m})$.

Step 3: Apply (9) with $m_\varphi(j,m)=(\ln b)^2\,\mathcal{L}^{(1)}_{\mathcal{R}f(\theta_{j,m},\cdot),b}(\sigma_{j,m})$, yielding the approximation of the inverse Radon transform $\mathcal{R}^{-1}$:

$$f_a(\mathbf{x})=\left(\left(\mathcal{B}_a^{-1}m_\varphi\right)\circ\varphi\right)(\mathbf{x}),\quad \mathbf{x}=(x_1,x_2)\in\mathbb{R}^2_+. \tag{20}$$

Indeed, according to (17)–(19), we have $m_\varphi(j,m)=(\ln b)^2\,\mathcal{L}^{(2)}_{f,b}(j+1,m+1)$, and after substituting $m_\varphi(j,m)$ into (9), and applying the bivariate Laplace transform inversion we obtain the approximation f_a of f.

4.2. Estimation of the probability density function given the projected data-set

Let $\mathbf{X}_i$, $i=1,\dots,n$, be a sequence of i.i.d. random vectors with probability density function (pdf) f. Suppose we are given only the projections $\langle\mathbf{X}_i,\boldsymbol{\xi}_\theta\rangle$, $i=1,\dots,n$, in the directions $\boldsymbol{\xi}_\theta\in S^2$. In [14] the uniform convergence rate of the empirical Radon transform and the rate in the L_2 -norm of its inversion were derived. In their approach, the authors first estimated the Radon transform $g=\mathcal{R}f$, and then the target pdf f based on the knowledge of $\langle\mathbf{X}_i,\boldsymbol{\xi}_\theta\rangle$, $i=1,\dots,n$, for all directions $\boldsymbol{\xi}_\theta\in S^2$ on the unit sphere in $\mathbb{R}^3$. They avoid the regularization procedure for recovering the inverse operator $\mathcal{R}^{-1}$ by assuming f to be a member of a class of rapidly decreasing C^∞-functions on $\mathbb{R}^3$ with unbounded support. In the case of $d=2$, when f has a compact support in $\mathbb{R}^2$, the singular value decomposition was applied in [5].

In this section, to estimate the Radon transform, consider the empirical Laplace transform of the data-set $\langle\mathbf{X}_i,\boldsymbol{\xi}_\theta\rangle$, $i=1,\dots,n$:

$$\widehat{\mathcal{L}}^{(1)}_{\langle\mathbf{X},\boldsymbol{\xi}_\theta\rangle,b}(\sigma):=\frac{1}{n}\sum_{i=1}^{n}e^{-\sigma(\ln b)\langle\mathbf{X}_i,\boldsymbol{\xi}_\theta\rangle} \tag{21}$$

representing the empirical counterpart of $\mathcal{L}^{(1)}_{\mathcal{R}f(\cdot,\theta),b}(\sigma)$, that is, according to (17) , equal to

$$\mathcal{L}^{(1)}_{\mathcal{R}f(\theta,\cdot),b}(\sigma)=\mathcal{L}^{(2)}_{f,b}(\sigma\cos\theta,\sigma\sin\theta),\quad \text{for } 0\le\theta\le 2\pi \text{ and } \sigma>0. \tag{22}$$

By substitution of the empirical Laplace transform $\widehat{\mathcal{L}}^{(1)}_{\langle\mathbf{X},\boldsymbol{\xi}_\theta\rangle,b}(\sigma)$ with $\sigma=\sigma_{j,m}$ and $\theta=\theta_{j,m}$ (defined according to (19)) into (20), where $\widehat{m}_\varphi(j,m)=(\ln b)^2\,\widehat{\mathcal{L}}^{(1)}_{\langle\mathbf{X},\boldsymbol{\xi}_{\theta_{j,m}}\rangle,b}(\sigma_{j,m})$, is used instead of $m_\varphi(j,m)$, we obtain the empirical version of Radon transform inversion:

$$\widehat{f}_a(\mathbf{x})=\left(\left(\mathcal{B}_a^{-1}\widehat{m}_\varphi\right)\circ\varphi\right)(\mathbf{x}),\quad \mathbf{x}=(x_1,x_2)\in\mathbb{R}^2_+, \tag{23}$$

In other words, according to our approach, we skip the step of estimating the Radon transform $g=\mathcal{R}f$, and use only the scaled values of the empirical Radon transform of the data-set $\langle\mathbf{X}_i,\boldsymbol{\xi}_\theta\rangle$, $i=1,\dots,n$, evaluated for several directions $\theta\in\{\theta_{j,m},(j,m)\in\mathbb{N}_\alpha\times\mathbb{N}_{\alpha'}\}$.

4.3. Approximating the Radon transform given the scaled values of $\mathcal{L}^{(2)}_f$

Assume θ is a fixed direction. Application of (17) in the opposite direction in combination with (16) and Corollary 1 leads to recovering the Radon transform $\mathcal{R}f(\theta,\cdot)$ itself. To be more specific, assume that the values of $\mathcal{L}^{(2)}_{f,b}$ are known. Evaluate its values $\mathcal{L}^{(2)}_{f,b}(\sigma\cos\theta,\sigma\sin\theta)$ with $\sigma=j+1$, for each $j=0,1,\dots,\alpha$. From (17) it follows that

$$\mathcal{L}^{(2)}_{f,b}((j+1)\cos\theta,(j+1)\sin\theta)=\mathcal{L}^{(1)}_{\mathcal{R}_f(\theta,\cdot),b}(j+1) \tag{24}$$

Hence, from the knowledge of $\mathcal{L}^{(1)}_{\mathcal{R}f(\theta,\cdot),b}(j+1)$ one can recover the Radon transform $\mathcal{R}f$ itself by applying the univariate Laplace transform inversion as stated in Corollary 1, where

$$m_\phi(j)=(\ln b)\,\mathcal{L}^{(2)}_{f,b}((j+1)\cos\theta,(j+1)\sin\theta). \tag{25}$$

The approximation of the Radon transform is constructed as follows:

$$\mathcal{R}f_\alpha(\theta,t)=\frac{(\ln b)\,\Gamma(\alpha+2)}{\Gamma([\alpha\phi(t)]+1)}\sum_{j=0}^{\alpha-[\alpha\phi(t)]}\frac{(-1)^j\mathcal{L}^{(2)}_{f,b}\left((j+1+[\alpha\phi(t)])\cos\theta,(j+1+[\alpha\phi(t)])\sin\theta\right)}{j!(\alpha-[\alpha\phi(x_1)]-j)!}, \tag{26}$$

for each $\theta\in(0,2\pi)$, $t>0$, and $\phi(t)=b^{-t}$.

Theorem 3. *If for each $\theta\in(0,2\pi)$, the function $\mathcal{R}f(\theta,\cdot)$ is continuous and bounded, then*

$$\mathcal{R}f_\alpha(\theta,\cdot)\xrightarrow{u}\mathcal{R}f(\theta,\cdot)\quad as\quad \alpha\to\infty.$$

Proof. The statement of theorem follows by combining (24)–(26) with (16) and Corollary 1, where instead of f we have $\mathcal{R}_f(\theta,\cdot)$. □

4.4. Two new estimates of the Radon transform

Some asymptotic properties of the kernel type estimate (the so-called empirical Radon transform) of $\mathcal{R}f$ have been studied in [14]. Here we suggest two new estimates. The first one could be used when the model is observed directly: assume that $\mathbf{X}_i$, $i = 1, \ldots, n$, is a sequence of i.i.d. random vectors in $\mathbb{R}^2$ having an unknown pdf f. The second estimate of $\mathcal{R}f$ is defined when only the projections of $\mathbf{X}_i$'s are available. In both cases our goal is to estimate the Radon transform of f.

Consider the empirical bivariate Laplace transform of the sample $\mathbf{X}_i$, $i = 1, \ldots, n$ that is scaled by $c = \ln b$:

$$\widehat{\mathcal{L}}^{(2)}_{\mathbf{X},b}(\mathbf{t}) = \frac{1}{n}\sum_{i=1}^{n} e^{-\langle c\mathbf{t}, \mathbf{X}_i\rangle}, \quad \mathbf{t} = (t_1, t_2). \tag{27}$$

Taking into account Eqs. (24)–(26), where the empirical version of the bivariate Laplace transform $\widehat{\mathcal{L}}^{(2)}_{\mathbf{X},b}$ is used instead of $\mathcal{L}^{(2)}_{f,b}$, one derives the following estimate of the Radon transform:

$$\widehat{\mathcal{R}}f_{\alpha,I}(\theta, t) = \frac{(\ln b)\,\Gamma(\alpha+2)}{\Gamma([\alpha\phi(t)]+1)} \sum_{j=0}^{\alpha-[\alpha\phi(t)]} \frac{(-1)^j \widehat{\mathcal{L}}^{(2)}_{\mathbf{X},b}\big((j+1+[\alpha\phi(t)])\cos\theta, (j+1+[\alpha\phi(t)])\sin\theta\big)}{j!(\alpha-[\alpha\phi(x_1)]-j)!}, \tag{28}$$

as $\alpha, n \to \infty$.

Now, assume that the following data is given: $\{\langle \mathbf{X}_i, \boldsymbol{\xi}_\theta\rangle\}_{i=1}^n$, i.e., the projections of the $\mathbf{X}_i$'s in direction $\boldsymbol{\xi}_\theta$ are known. If we substitute, instead of $\mathcal{L}^{(1)}_{f,b}(\sigma)$, the empirical Laplace transform of the data $\widehat{\mathcal{L}}^{(1)}_{\langle \mathbf{X}, \boldsymbol{\xi}_\theta\rangle, b}(\sigma)$ defined in (21), into (15) and (16), we obtain the second estimate of the Radon transform:

$$\widehat{\mathcal{R}}f_{\alpha,II}(\theta, t) = \frac{(\ln b)\,\Gamma(\alpha+2)}{\Gamma([\alpha\phi(t)]+1)} \sum_{j=0}^{\alpha-[\alpha\phi(t)]} \frac{(-1)^j \widehat{\mathcal{L}}^{(1)}_{\langle \mathbf{X}, \boldsymbol{\xi}_\theta\rangle, b}\big((j+1+[\alpha\phi(t)])\big)}{j!(\alpha-[\alpha\phi(x_1)]-j)!}. \tag{29}$$

On the other hand, substituting the values of the empirical Laplace transform of the data $\widehat{\mathcal{L}}^{(1)}_{f,b}$ into (29) and changing the order of summations yields another representation of the estimate:

$$\widehat{\mathcal{R}}f_{\alpha,B}(\theta, t) = \frac{1}{n}\sum_{i=0}^{n} \frac{(\ln b)\,\Gamma(\alpha+2)\phi\big(\langle \mathbf{X}_i, \boldsymbol{\xi}_\theta\rangle\big)^{[\alpha\phi(t)]+1}\big(1-\phi(\langle \mathbf{X}_i, \boldsymbol{\xi}_\theta\rangle)\big)^{\alpha-[\alpha\phi(t)]}}{\Gamma([\alpha\phi(t)]+1)\,\Gamma(\alpha-[\alpha\phi(t)]+1)}. \tag{30}$$

This estimate $\widehat{\mathcal{R}}f_{\alpha,B}$ represents the asymmetric kernel density construction when the kernels are specified by the Beta densities.

Remark 5. Note that when data represents the observations $\mathbf{X}_i$, $i = 1, \ldots, n$, sampled directly from f, then the estimates, introduced in (28) and (29) coincide. Indeed, it is sufficient to note that the empirical version of Eq. (24), written in terms of the empirical counterparts $\widehat{\mathcal{L}}^{(2)}_{f,b}$ and $\widehat{\mathcal{L}}^{(1)}_{<\mathbf{X}, \boldsymbol{\xi}_\theta>, b}$ is also valid.

5. Numerical implementation

In this section we demonstrate the performance of the approximated and estimated inversions of the Laplace and the Radon transforms for several bivariate distributions and functions. The plots of the recovered Radon transform $\mathcal{R}f$ are provided as well.

Example 1. Let $\mathbf{X} = (X, Y)$ be a bivariate vector with independent components exponentially distributed with rates $\beta_1 = 2$ and $\beta_2 = 2$, respectively. The bivariate scaled Laplace transform is

$$\mathcal{L}^{(2)}_f(s\ln b, t\ln b) = \frac{\beta_1}{\beta_1 + s\ln b} \times \frac{\beta_2}{\beta_2 + t\ln b}. \tag{31}$$

Fig. 1 shows the true density function f and its approximation f_a. We set $\alpha = \alpha' = 32$, $b = 1.35$. The functions were evaluated on the grid

$$(x_i, y_j) = \left[\frac{1}{\ln b}\ln\left(\frac{\alpha}{\alpha - i + 1}\right), \frac{1}{\ln b}\ln\left(\frac{\alpha'}{\alpha' - j + 1}\right)\right]; \ i = 1, \ldots, \alpha \text{ and } j = 1, \ldots, \alpha'.$$

Example 2. Let $\mathbf{X} = (X, Y)$ be a random vector with independent components distributed according to the Gamma distributions: $X \sim \text{Gamma}(a_1, \beta_1)$ and $Y \sim \text{Gamma}(a_2, \beta_2)$. The bivariate scaled Laplace transform of (X, Y) is given by

$$\mathcal{L}^{(2)}_f(s\ln b, t\ln b) = \left(\frac{1}{\beta_1 s\ln b + 1}\right)^{a_1}\left(\frac{1}{\beta_2 t\ln b + 1}\right)^{a_2}. \tag{32}$$

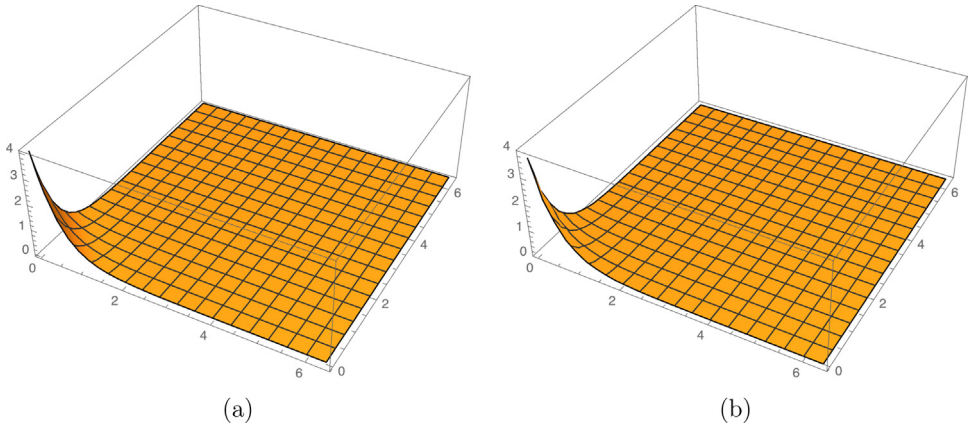

Fig. 1. (a) The true density f when $\mathbf{X} \sim 4e^{-(2x+2y)}$; and (b) Approximation f_a with $\alpha = \alpha' = 32$, $b = 1.35$.

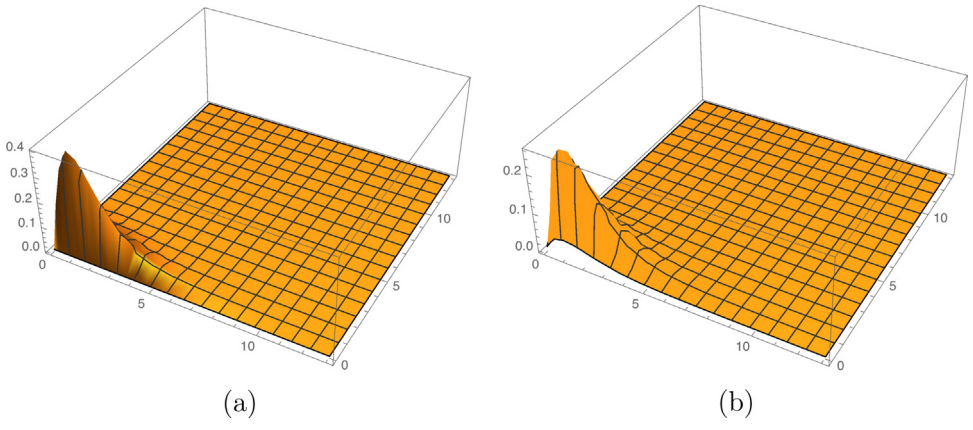

Fig. 2. (a) The true density of $\mathbf{X} \sim$ Gamma(2, 1) $\times$ Gamma(2.5, 0.4); and (b) Approximation f_a with $\alpha = 50$, $\alpha' = 60$, $b = 1.35$.

Substitution of (32) into (9) provides the approximate the joint density function of (X_1, X_2):

$$f_a(x,y) = \frac{\ln^2 b\, \Gamma(\alpha+2)\Gamma(\alpha'+2)}{\Gamma([\alpha\phi(x)]+1)\Gamma([\alpha'\phi(y)]+1)} \times \sum_{m=0}^{\alpha-[\alpha\phi(x)]} \sum_{l=0}^{\alpha'-[\alpha'\phi(y)]} \frac{(-1)^{m+l}}{m!l!(\alpha-[\alpha\phi(x)]-m)!(\alpha'-[\alpha' b^{-y}]-l)!} \times \left(\frac{1}{\beta_1(m+1+[\alpha\phi(x)])\ln b+1}\right)^{a_1} \left(\frac{1}{\beta_2(l+1+[\alpha'\phi(y)])\ln b+1}\right)^{a_2}.$$

Consider the case where $\{a_1 = 2, \beta_1 = 1, a_2 = 2.5, \beta_2 = 0.4\}$. We set-up $\alpha = 50, \alpha' = 60$ and $b = 1.35$. From Fig. 2 we can say that our approximation is quite close to the true f.

Example 3. Assume that a random vector $\mathbf{X}$ follows the Downton Bivariate Exponential distribution – $DBVE(\mu_1, \mu_2, \rho)$ introduced by Downton [17]. The corresponding density function is given by

$$f(x,y) = \frac{\mu_1\mu_2}{1-\rho} \exp\left(-\frac{\mu_1 x + \mu_2 y}{1-\rho}\right) I_0\left(\frac{2\sqrt{\rho\mu_1\mu_2 xy}}{1-\rho}\right), \ (x,y) \in \mathbb{R}^2_+,$$

where $I_0(\cdot)$ is the Bessel function of the first kind, $\mu_1,\ \mu_2 \geq 0$, and $0 \leq \rho \leq 1$. The bivariate scaled Laplace transform of (X, Y) is given by

$$\mathcal{L}_f^{(2)}(s\ln b, t\ln b) = \frac{\mu_1\mu_2}{(\mu_1 + s\ln b)(\mu_2 + t\ln b) - \rho\, s\, t \ln^2 b}.$$

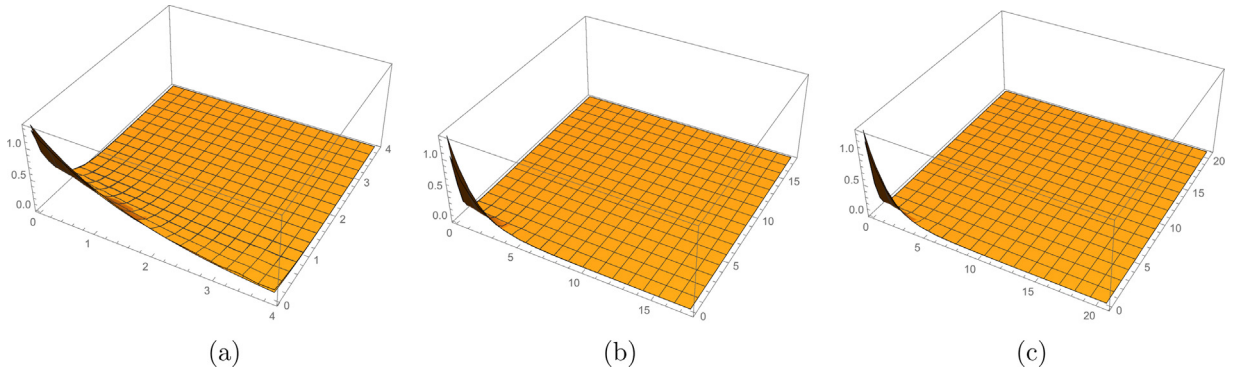

Fig. 3. The true density f of $\mathbf{X} \sim DBVE(1/2, 2, 1/4)$ and approximated f_a; (a) with $\alpha = \alpha' = 50$, $b = \exp(1)$; (b) with $\alpha = \alpha' = 50$, $b = 1.25$; and (c) with $\alpha = \alpha' = 100$, $b = 1.25$.

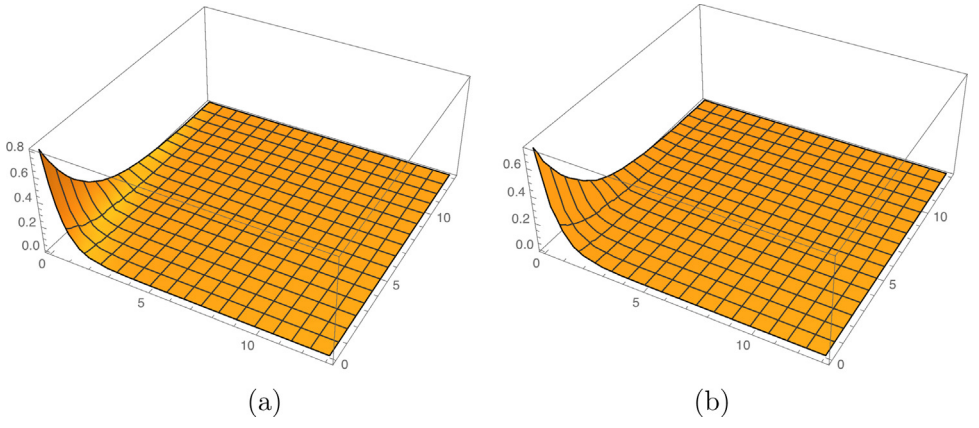

Fig. 4. (a) The true pdf f of $\mathbf{X} \sim DBVE(2, 1/2, -1/4)$; and (b) approximated pdf f_a with $\alpha = \alpha' = 32$, $b = 1.45$.

Again, the approximated joint density function of (X, Y) is obtained by substituting the bivariate scaled Laplace transform into (9).

We studied the behavior of the approximation $f_a(x, y)$ with different values of parameters involved in this construction. For illustration, two cases with parameter choices $\{\mu_1 = 1/2, \mu_2 = 2, \rho = 1/4\}$ and $\{\mu_1 = 2, \mu_2 = 1/2, \rho = -1/4\}$ are considered. The first case is borrowed from [18]. Corresponding approximations with two different values of parameters $\alpha = \alpha'$ and with the same b value of $b = 1.25$, are displayed in Fig. 3, see plots (b) and (c).

It is worth mentioning that a comparison of the construction, similar to (9), where the parameter $b = \exp(1)$, was conducted in [18]. They established that the method based on the Laguerre polynomial expansion technique produces a slightly better approximation if compared to (9) when $b = \exp(1)$. Our simulation study justifies the observation that taking the values of $b > 1$ closer to 1 produces more accurate approximation of f if it has a heavy tail on the right.

In other words, by introducing an extra parameter $1 < b \leq \exp(1)$ our method provides more accurate approximations when compared to the one based on the fixed value of $b = \exp(1)$. See Fig. 3(a), where we set-up $\alpha = \alpha' = 50$ and $b = \exp(1)$ and compare it with plot (b), where $b = 1.25$. This phenomena was also observed in other examples considered below, where we evaluated corresponding approximations with $b < \exp(1)$. For example, Fig. 4 displays the surfaces of true and approximated densities with $\alpha = \alpha' = 32$ and $b = 1.45$. Comparing the true joint density functions with their approximates, we see that the approximations are relatively close to the true distributions.

Example 4. Let us approximate the Radon transform of the function $f(x, y) = xy$, $(x, y) \in \mathbb{R}^2_+$, given the scaled values of its Laplace transform. Recall that

$$\mathcal{L}_f^{(2)}(s \ln b, t \ln b) = \frac{1}{(s \ln b)^2} \times \frac{1}{(t \ln b)^2}$$

and

$$\mathcal{R}f(\theta, t) = \frac{2t^3}{3 \sin(2\theta)}, \quad (\theta, t) \in (0, \pi/2) \times \mathbb{R}_+.$$

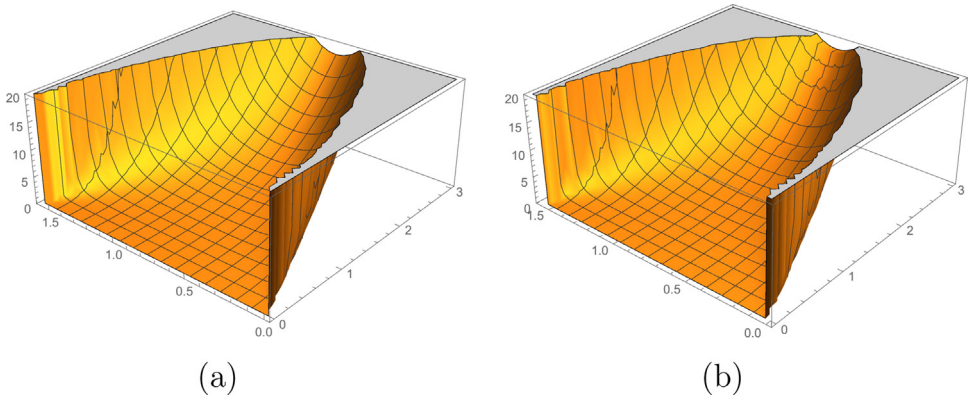

Fig. 5. (a) The true Radon transform $\mathcal{R}f(\theta,t)$ when $f(x,y)=xy$; (b) Approximated $\mathcal{R}f_\alpha(\theta,t)$ when $\alpha=100$, $b=2.15$, and $(\theta,t)\in(0,\pi/2)\times(0,3)$.

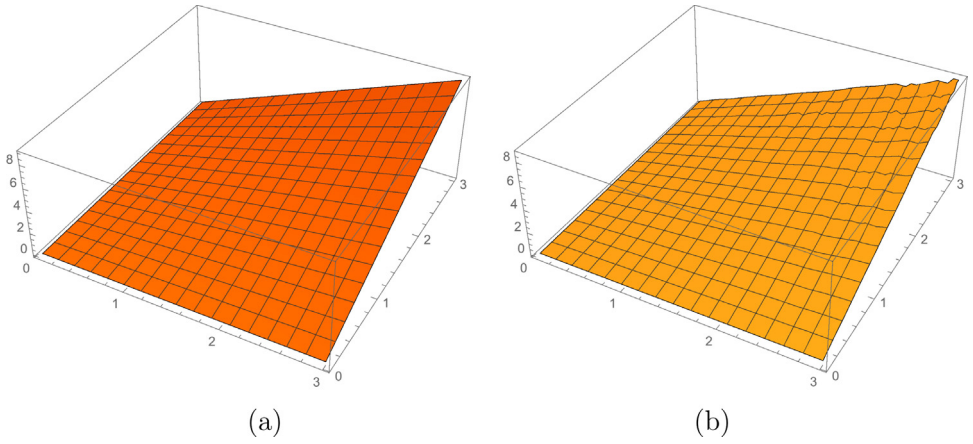

Fig. 6. (a) True function $f(x,y)=xy$; (b) Approximated Radon transform inversion $f_a(x,y)$ when $\alpha=\alpha'=60$, $b=1.95$ and $(x,y)\in[0,3]^2$.

According to (22), the scaled value of the Laplace transform of $\mathcal{R}f(\theta,\cdot)$ is related to $\mathcal{L}_f^{(2)}(\cdot,\cdot)$. Hence, to recover $\mathcal{R}f$, we can apply (26) with

$$(\ln b)\mathcal{L}^{(1)}_{\mathcal{R}f(\theta,\cdot),b}(j+1)=(\ln b)\mathcal{L}^{(2)}_{f,b}((j+1)\cos\theta,(j+1)\sin\theta)=\frac{\ln b}{((j+1)\ln b\cos\theta)^2}\cdot\frac{1}{((j+1)\ln b\sin\theta)^2}. \tag{3}$$

See Fig. 5, where the Radon transform $\mathcal{R}f(\theta,t)$ of the function $f(x,y)=xy$, introduced in Example 4, as well as its approximation $\mathcal{R}f_\alpha(\theta,t)$ are plotted when $\alpha=100, b=2.15$. Now, let us recover the function $f(x,y)=xy$, given the values of its Radon transform $\mathcal{R}f$. Namely, let us evaluate the values of Radon transform in the direction $\theta_{j,m}$ and the values of Laplace transform of $\mathcal{R}f$ with argument $\sigma_{j,m}$, specified according to (19). We obtain the approximation f_a (see (20)). Fig. 6 displays the approximation $f_a(x,y)$ when $\alpha=\alpha'=60$, $b=1.95$ and $(x,y)\in[0,3]^2$.

Example 5. Let us estimate the Radon transform of the function $f(x,y)=e^{-x-y},(x,y)\in\mathbb{R}^2_+$, given the sample (X_i,Y_i), $i=1,\dots,n$, of size $n=1000$ of *i.i.d.* random vectors from f. See Fig. 7, where the curves of the estimated density $\widehat{f}_a(x,y)$ and the target function $f(x,y)=e^{-x-y}$ are displayed. Here, $\alpha=\alpha'=30, b=1.95$. Note that in this example,

$$\mathcal{R}f(\theta,t)=\frac{1}{\cos\theta-\sin\theta}\left[e^{-\frac{t}{\cos\theta}}-e^{-\frac{t}{\sin\theta}}\right],\quad\text{for}\quad(\theta,t)\in(0,\pi/2)\times\mathbb{R}_+. \tag{13}$$

The Radon transform $\mathcal{R}f(\theta,t)$ of the function $f(x,y)=e^{-x-y}$ is plotted in Fig. 8(a), while in Fig. 8(b) the approximated $\mathcal{R}f_\alpha(\theta,t)$ defined in (26) is displayed when $\alpha=60, b=1.95125$. In Fig. 9 we plotted two estimates: for $\widehat{\mathcal{R}f}_{\alpha,II}(\theta,t)$, see plot (a), and for $\widehat{\mathcal{R}f}_{\alpha,B}(\theta,t)$, see plot (b), respectively. In both plots we took $(\theta,t)\in(0,\pi/2)\times(0,4)$. To evaluate the estimates $\widehat{\mathcal{R}f}_{\alpha,II}$ and $\widehat{\mathcal{R}f}_{\alpha,B}$, we set-up $n=1000, \alpha=30, b=1.95$. We can see that all four surfaces are very similar to each other.

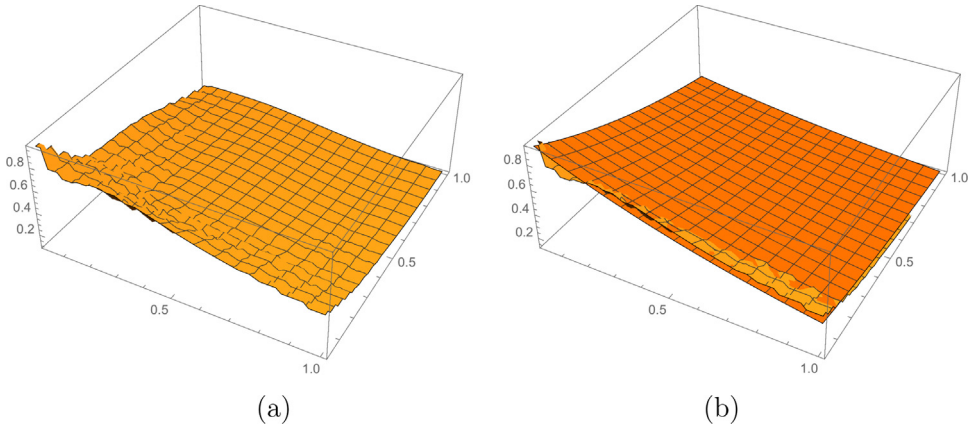

Fig. 7. (a) Estimated function $\widehat{f}_a(x, y)$ based on the Radon transform inversion (23), when $n = 1000$ and $\alpha = \alpha' = 30$, $b = 1.95$, and $(x, y) \in [0, 1]^2$; (b) Estimated $\widehat{f}_a(x, y)$ and the true function $f(x, y) = e^{-x-y}$.

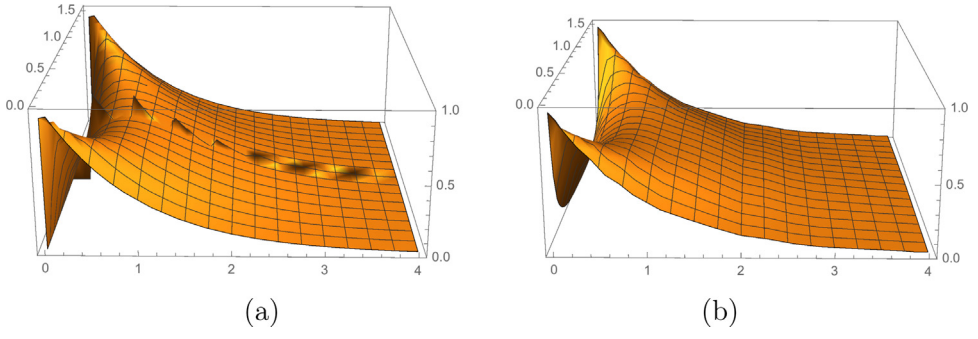

Fig. 8. (a) The Radon transform $\mathcal{R}f(\theta, t)$ of $f(x, y) = e^{-x-y}$; (b) Approximated Radon transform $\mathcal{R}f_\alpha(\theta, t)$ defined by (26) when $\alpha = 60$, $b = 1.95125$. In both cases $(\theta, t) \in (0, \pi/2) \times (0, 4)$.

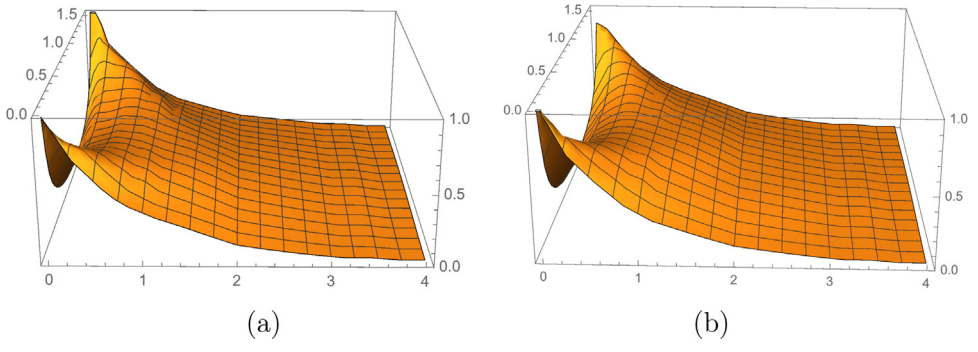

Fig. 9. (a) The estimates of $\mathcal{R}f(\theta, t)$ by (a) $\widehat{\mathcal{R}}f_{\alpha,II}(\theta, t)$ defined in (29); and (b) $\widehat{\mathcal{R}}f_{\alpha,B}(\theta, t)$ defined in (30). In both cases $n = 1000$, $\alpha = 30$, $b = 1.95$, and $(\theta, t) \in (0, \pi/2) \times (0, 4)$.

6. Conclusion

Two new approximations, as well as estimates, of the underlying function, obtained from the scaled values of its Laplace and Radon transforms are proposed.

Our Methods have at least three advantages: (a) they are based on the knowledge of a finite number of the scaled values of Laplace and Radon transforms when the arguments of transforms are chosen from the lattice $\{(j + 1, m + 1) \ln b, 0 \le j \le \alpha,\ 0 \le m \le \alpha'\}$, and from a finite number of directions in the case of Radon transform inversion; (b) the proposed constructions admit very simple and closed form expressions; and (c) approximates are computationally stable without applying a regularization procedure. The parameters $\alpha \in \mathbb{N}_+$ and $\alpha' \in \mathbb{N}_+$ specify the total number of values of Laplace

or Radon transforms used in the proposed constructions. From the simulation study we conclude that increasing α and α' leads to better approximations. The choice of parameter b depends on the tail behavior of the underlying function: for functions with heavy tails smaller value of $b > 1$ is recommended. Finally, it is worth mentioning that the estimates of the Laplace and Radon transform inversions are obtained by substituting the empirical counterparts of the corresponding transforms. The problem of specifying the parameter $a = (\alpha_n, \alpha'_n)$ as a function of the sample size $n \to \infty$ requires conducting deeper analysis, and will be studied in a separate article.

Acknowledgments

This work was supported by the MERF-19 grant of the Department of Mathematics (WVU) and by the grant of MES State Committee of Science of the Republic of Armenia, in the frames of the research project 18T-1A252. The authors would like to thank the referees for their helpful suggestions, and Farhad Jafari for fruitful discussions that improved the presentation of the paper.

Appendix A. Supplementary data

In Section 5, to evaluate the approximations of the Laplace and Radon transforms inverses, as well as the Radon transform $\mathcal{R}f$ itself (defined in (9), (20), and (26), respectively), the package of Wolfram Mathematica has been used. In particular, to reproduce the plots from Figs. 4–6, the codes in Supplementary data are presented.

Supplementary material related to this article can be found online at https://doi.org/10.1016/j.cam.2021.113557.

References

[1] S.R. Deans, The Radon Transform and Some of its Applications, Wiley, New York, 1983.
[2] F. Natterer, F. Wübbeling, Mathematical Methods in Image Reconstruction, SIAM, Philadelphia, 2001.
[3] E.T. Quinto, An introduction to X-ray tomography and radon transform, Proc. Symp. Appl. Math. 63 (2006) 1–23.
[4] P. Kuchment, L.A. Kunyansky, Mathematics of thermoacoustic and photoacoustic tomography, in: Otmar Scherzer (Ed.), Handbook of Mathematical Methods in Imaging, Springer Verlag, ISBN: 978-0-387-92920-0, 2011, pp. 817–865, 1688 pp.
[5] I.M. Johnstone, B.W. Silverman, Speed of estimation in positron emission tomography and related inverse problems, Ann. Statist. 18 (1990) 251–280.
[6] P. Milanfar, W. Karl, A.S. Willsky, Recovering the Moments of a Function from Its Radon-Transform Projections: Necessary and Sufficient Conditions, Tech. Report, LIDS-P, No 2113, 1992, pp. 1–7.
[7] P. Milanfar, W. Karl, A.S. Willsky, A moment-based variational approach to tomographic reconstruction, IEEE Trans. Image Process. 5 (1996) 459–470.
[8] H. Choi, F. Jafari, V. Ginting, R. Mnatsakanov, Modified Radon transform inversion using moments, J. Inverse Ill-Posed Probl. 28 (1) (2020) 1–15, http://dx.doi.org/10.1515/jiip-2018-0090.
[9] R.M. Mnatsakanov, S. Li, The Radon transform inversion using moments, Statist. Probab. Lett. 83 (2013) 936–942.
[10] R.H. Aramyan, Generalized Radon transform on the sphere, Analysis 30 (3) (2010) 271–284.
[11] P. Milanfar, Geometric Estimation and Reconstruction from Tomographic Data (PhD dissertation), Massachusetts Institute of Technology, 1993.
[12] A.B. Goncharov, Methods of Integral Geometry and recovering a function with compact support from its projections in unknown directions, Acta Appl. Math. 11 (1988) 213–222.
[13] Yu.P. Petrov, V.S. Sizikov, Well-Posed, Ill-Posed, and Intermediate Problems with Applications, Konikijke Brill NV, Leiden, 2005.
[14] D.S. Gilliam, P. Hall, F.H. Ruymgaart, Rate of convergence of the empirical Radon transform, J. Multivariate Anal. 44 (1993) 115–145.
[15] R.M. Mnatsakanov, Moment-recovered approximations of multivariate distributions: The Laplace transform inversion, Statist. Probab. Lett. 81 (2011) 1–7.
[16] R.M. Mnatsakanov, K. Sarkisian, A note on recovering the distributions from exponential moments, Appl. Math. Comput. 219 (2013) 8730–8737.
[17] F. Downton, Bivariate exponential distributions in reliability theory, J. R. Stat. Soc. 32 (1970) 408–417.
[18] P.O. Goffard, S. Loisel, D. Pommeret, Polynomial approximations for bivariate aggregate claims amount probability distributions, Methodol. Comput. Appl. Probab. 19 (2017) 151–174.